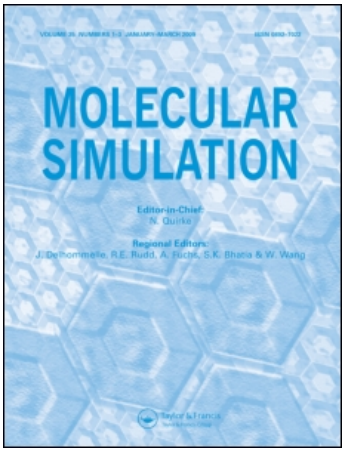

Molecular Simulation
Publication details, including instructions for authors and subscription information:
http://www.informaworld.com/smpp/title~content=t713644482

Adsorption of methanoic acid onto the low-index surfaces of calcite and aragonite

T. G. Cooper[a]; N. H. de Leeuw[a]
[a] Department of Chemistry, University of Reading, Reading, UK

Online publication date: 26 October 2010

To cite this Article Cooper, T. G. and de Leeuw, N. H.(2002) 'Adsorption of methanoic acid onto the low-index surfaces of calcite and aragonite', Molecular Simulation, 28: 6, 539 — 556
To link to this Article: DOI: 10.1080/08927020290030125
URL: http://dx.doi.org/10.1080/08927020290030125

Molecular Simulation, 2002 VOL. 28 (6-7), pp. 539–556

ADSORPTION OF METHANOIC ACID ONTO THE LOW-INDEX SURFACES OF CALCITE AND ARAGONITE

T.G. COOPER* and N.H. DE LEEUW

Department of Chemistry, University of Reading, Reading RG6 6AH, UK

(Received April 2001, accepted August 2001)

We have employed atomistic simulation techniques to investigate the effect of the adsorption of methanoic acid on the surfaces of calcite and aragonite. We have calculated surface energies and adsorption energies for all the surfaces considered, and compared the surface energies with those of the pure surfaces. Generally the methanoic acid molecules coordinate via their doubly bonded oxygen atom to surface calcium atoms, with the hydroxyl hydrogen atom directed towards oxygen atoms of surface carbonate groups. The hydrogen bonded to the carbon atom of the methanoic acid is usually pointing away from the surface, which is of considerable significance since we are using methanoic acid as a model adsorbate for long chain carboxylic acids, that are used extensively in the process of flotation. We suggest that the replacement of the hydrogen atom of the methanoic acid with a long chain hydrocarbon would not result in significantly different interactions and, thus, would give similar adsorption energies (-54 to $-113\,\mathrm{kJ\,mol^{-1}}$ on calcite, -40 to $-83\,\mathrm{kJ\,mol^{-1}}$ on aragonite)

Keywords: Calcite; Aragonite; Adsorption; Methanoic acid; Calcium carbonate

INTRODUCTION

Calcium carbonate is one of the most abundant minerals and important in many fields, for example as an environmental sink due to its strong surface interactions with heavy metals in the environment [1]; in industrial water treatment [2], due to its tendency to form scale in boilers and pipes, and as the building block of shells

*Corresponding author. E-mail: t.g.cooper@reading.ac.uk.

ISSN 0892-7022
DOI: 10.1080/08927020290030125

and skeletons [3]. As such, the different polymorphs, in particular calcite, have been the subject of extensive and varied research, both experimentally and theoretically.

The surface structure has been studied by a variety of methods, such as SEM studies of the calcite $\{10\bar{1}4\}$ and $\{10\bar{1}1\}$ surfaces in ultrahigh vacuum [4,5] and in air with SFM, e.g. in studies of step growth on the $\{10\bar{1}4\}$ surface [6]. AFM investigations under aqueous conditions have been carried out to investigate a host of features, such as distinct relaxation of surface oxygen atoms on the $\{10\bar{1}4\}$ plane [7], and the role of steps and spiral dislocations in crystal growth [8]. Recent theoretical research has included modelling the relaxation of the $\{10\bar{1}4\}$ calcite surface under wet and dry conditions [9], modelling the competitive adsorption of water and methanoic acid onto the $\{10\bar{1}4\}$ surface of calcite [10], crystal dissolution from step edges [11], and the formation and growth of rhombohedral pits on the $\{10\bar{1}4\}$ surface [12,13].

Due to the omnipresence of carbon-containing molecules in the environment, the adsorption of a number of organic molecules onto the surfaces of calcite have been studied experimentally, e.g. the adsorption of stearate monolayers onto the surface of calcite by X-ray reflectivity techniques [14]. From this study, important aspects of the *in situ* structure, bonding, adsorption and growth mechanisms have been determined, which are of considerable significance in geochemical reaction and transport processes. In addition, the adsorption of polar aromatic hydrocarbons, specifically benzoic acid, benzyl alcohol and benzylamine, onto the surfaces of calcite has been studied by adsorption experiments, due to their importance in the wettability of hydrocarbon reservoirs [15].

Calcium carbonate is often found together with calcium fluoride in mineral deposits and it is, therefore, important to investigate potentially selective surfactants for their separation in mineral separation processes. The process of flotation is used extensively in the mining industry [16,17] and is based on the selective adsorption of collectors (surfactants) to the mineral of interest, thus giving it a hydrophobic surface [18,19], after which the particles can be separated from the mixture. One of the major surfactants used in industrial flotation processes is oleic acid [20–22]. In this study, we use atomistic simulation techniques to investigate the adsorption of methanoic acid on the low index surfaces of calcite and aragonite as this adsorbate has the same functional group as oleic acid, but without the hydrocarbon chain. Thus, we can concentrate on the interactions (mainly electrostatic) between surfaces and functional group, which are thought to be the main contributory factor in the adsorption process [23]. Experimentally, it is often difficult to determine the fundamental interactions that take place in the separation process. Now, with atomistic simulation techniques capable of modelling the structure of mineral surfaces at the atomic level, it is

possible to study computationally the interactions between the crystal surface and the adsorbates. These modelling techniques have been shown to accurately predict structures and properties of a wide range of minerals, including crystal morphology [24–26], surface structure [27–29] and adsorption behaviour [30–32].

METHODS

We employ atomistic simulation techniques, based on the Born model of solids [33], to model the geometries and energies of the calcium carbonate surfaces. The Born model of solids assumes that the ions in the crystal interact via long-range electrostatic forces and short-range forces, including both the repulsions and the van der Waals' attractions between neighbouring electron charge clouds. The electronic polarisability of the atoms is included via the shell model of Dick and Overhauser [34] where each polarisable atom, in our case oxygen, is represented by a core and a massless shell, connected by a spring. The polarisability of the atom is then determined by the spring constant and the charges of the core and shell. The potential parameters used in this work are those derived empirically by Pavese *et al*. [35] in their study of the thermal dependence of structural and elastic properties of calcite. The general cvff potential parameters [36] are used to describe the methanoic acid molecules, while the interactions between the mineral surfaces and methanoic acid molecules are those derived by de Leeuw *et al*. [10].

We employed the static energy minimisation code METADISE [37] which is designed to model dislocations, surfaces and interfaces. This code follows the approach of Tasker[38], where the crystal consists of two blocks, each comprising two regions, and periodic in two dimensions. Region I contains those atoms near the extended defect, in this case the surface layer and a few layers immediately below, where the ions are allowed to relax to their mechanical equilibrium. Region II contains those atoms further away and represents the rest of the crystal. Although the ions in this region are held at their bulk equilibrium positions, region II is allowed to move with respect to region I. Both regions I and II need to be sufficiently large for the energy to converge. The bulk crystal is modelled by both blocks together, while one block simulates the surface.

The surface energy, γ, is defined as

$$\gamma = \frac{(U_s - U_b)}{A} \tag{1}$$

where U_s is the energy of the surface block, U_b is the energy of the bulk crystal containing the same number of atoms as the surface block and A is the surface

area. The surface energy is a measure of the thermodynamic stability of the surface with a low positive value indicating a stable surface.

The adsorption energies were calculated by comparing the energy of the surface with adsorbed species with that of the sum of the pure surface and the energy of an isolated methanoic acid molecule.

$$U_{\text{ads}} = U_{\text{s+HCOOH}} - (U_{\text{s}} + U_{\text{HCOOH}}) \tag{2}$$

where U_{ads} is the adsorption energy, $U_{\text{s+HCOOH}}$ is the energy of the surface with adsorbed methanoic acid, and U_{HCOOH} is the energy of a methanoic acid molecule. The energy of the methanoic acid molecule is made up of two parts; its self energy, calculated to be -19.8 eV, and its experimental hydration energy of -0.49 eV [39]. The methanoic acid is adsorbed onto the surfaces from solution and, hence, this latter term needs to be taken into account when calculating the surface and adsorption energies.

Experimentally, the surface energy is the energy required to cleave a crystal, thus exposing the surface. The low Miller index surfaces are the closest packed and, hence, have the smallest surface area per unit cell. As the unit cell volume is fixed, these low index surfaces have the largest interplanar spacing and for that reason are usually easily cleaved, generating the lowest surface energies. We have, therefore, considered five low index surfaces of calcite, all of which are important in the experimental morphology, including the $\{10\overline{1}4\}$ surface which is the major cleavage plane of calcite. For aragonite, we considered the seven lowest index surfaces, including the {010}, {011} and {110} surfaces, which are generally the surfaces expressed in the experimental morphology. The surfaces were cut in such a way as to keep carbonate groups intact. Two of the calcite surfaces were dipolar containing more than one termination; a calcium and a carbonate terminated plane. The dipoles were removed by the introduction of surface vacancies before relaxation and adsorption of methanoic acid. Most of the aragonite surfaces also had more than one termination and all different terminations of the calcite and aragonite surfaces were considered in the calculations.

The methanoic acid molecules were adsorbed in a series of partial coverages up to full monolayer coverage. As the surface areas of the different surfaces considered in this work vary, we need to determine a consistent way of describing the surface coverage. Aragonite has a more open structure than calcite and its interatomic distances at the surface (Ca–Ca, Ca–O, O–O distances) are, therefore, larger than in calcite. In addition, as described above, surfaces of low Miller index have smaller surface areas than those of higher indices. By full monolayer coverage, we therefore mean that no more methanoic acid molecules can be adsorbed onto the surface without the formation of a second layer and we

will express the coverage on each surface as the number of molecules of methanoic acid per surface area. In addition to varying the adsorbate coverage, various initial orientations of the methanoic acid molecules were considered to ensure that, as far as possible, the lowest energy configuration was found. The methanoic acid molecules were brought down onto the surface, after which the surface and adsorbed molecules were allowed to relax.

RESULTS AND DISCUSSION

We shall consider the reactions between the methanoic acid molecules and the surface atoms, in particular the hydroxyl hydrogen of the methanoic acid (O–H), the hydrogen bonded to the carbon atom (C–H) the doubly bonded oxygen (C = O), and the oxygen of the hydroxyl group (C–O).

Calcite

Calcite has a rhombohedral crystal structure with space group $R\bar{3}c$ and $a = b = 4.990$ Å, $c = 17.061$ Å, $\alpha = \beta = 90°$ and $\gamma = 120°$ which on energy minimisation relaxed to $a = b = 4.797$ Å, $c = 17.482$ Å, $\alpha = \beta = 90°$ and $\gamma = 120°$. In addition to the major $\{10\bar{1}4\}$ surface, we also studied the $\{0001\}$, $\{10\bar{1}0\}$, $\{10\bar{1}1\}$ and $\{11\bar{2}0\}$ surfaces. The surface structures of the pure surfaces have been described extensively in previous work [26,31] and in this work we concentrate on describing the surfaces after adsorption of methanoic acid. The surface and adsorption energies are listed in Table I.

All the calcite surfaces considered were stabilised considerably by the adsorption of methanoic acid. On the $\{10\bar{1}4\}$ and calcium terminated $\{0001\}$ surfaces, a maximum adsorption of three methanoic acid molecules per unit cell

TABLE I Surface energies for pure calcite surfaces and after adsorption of methanoic acid

	Surface energy ($J\,m^{-2}$)			
Surface	Pure surface	After adsorption of methanoic acid	Coverage (no. $HCOOH\,nm^{-2}$)	Adsorption energy ($kJ\,mol^{-1}$)
$\{10\bar{1}4\}$	0.59	0.24	3.9	−54.44
$\{10\bar{1}1\}Ca$	0.98	0.72	3.5	−44.81
$\{10\bar{1}1\}CO_3$	1.00	0.48	3.5	−90.06
$\{11\bar{2}0\}$	1.39	0.62	4.1	−112.92
$\{10\bar{1}0\}$	0.97	0.73	2.4	−61.16
$\{0001\}Ca$	0.97	0.56	3.8	−64.73
$\{0001\}CO_3$	0.98	0.53	5.0	−54.70

was achieved, while on all the other surfaces four methanoic acid molecules could be adsorbed per cell. It is clear from Table I, though, that the maximum coverages per surface area are fairly constant across the range of surfaces.

The $\{10\bar{1}4\}$ surface remains the most stable surface after adsorption of methanoic acid, with a surface energy of $0.24\,\mathrm{J\,m^{-2}}$. The methanoic acid molecules coordinate via their C = O oxygen atom to surface calcium atoms at distances ranging from 2.21 to 2.26 Å. The O–H hydrogen atoms are coordinated to oxygen atoms of surface carbonate groups at distances of between 2.41 and 2.52 Å, and the C–H hydrogen atoms point away from the surface. Fig. 1 shows the relaxed $\{10\bar{1}4\}$ surface with a full monolayer of adsorbed methanoic acid molecules.

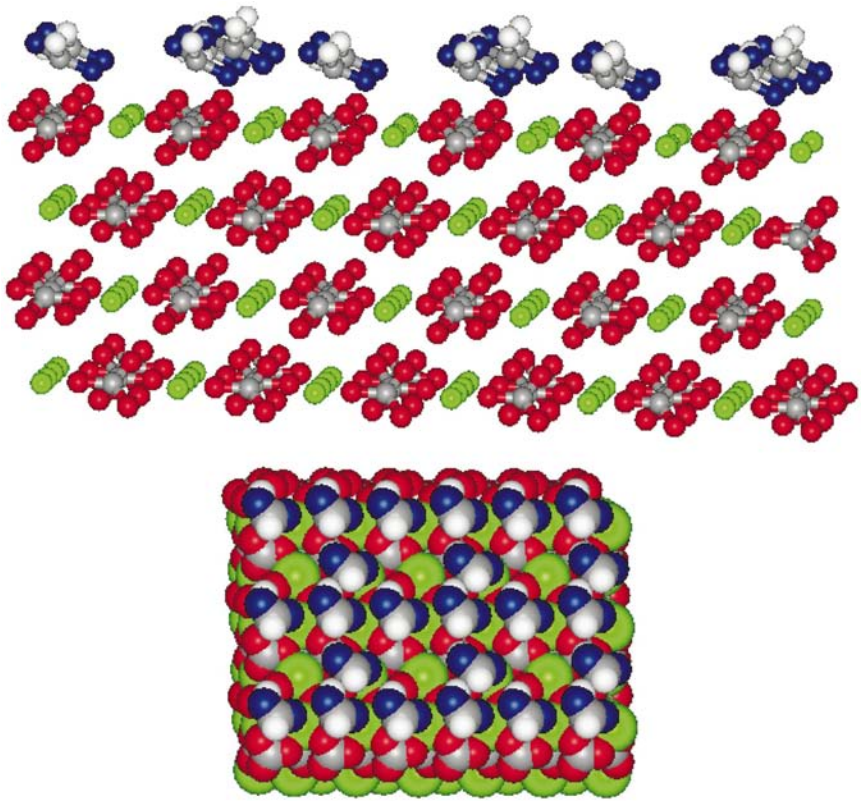

FIGURE 1 (a) Side view. (b) Plan view of the relaxed structure of the calcite $\{10\bar{1}4\}$ surface with adsorbed methanoic acid molecules. Key: Ca = green; C = grey; O (carbonate) = red; O (methanoic acid) = blue; and H = white.

The next two most stable surfaces are the carbonate terminated {0001} and {10$\bar{1}$1} surfaces. From Table I, we see that there is now a distinct preference for the carbonate terminated dipolar surfaces over the corresponding calcium terminated ones. Although the pure surface terminations were equally stable, upon adsorption of methanoic acid the carbonate-terminated surfaces have become more stable than the calcium terminated ones. On the calcium terminated {0001} plane ($0.56\,J\,m^{-2}$), the methanoic acid molecules again coordinate via their C = O oxygen atom to surface calcium atoms. However, due to the dipolar nature of the surfaces, 50% of the surface calcium positions (or carbonate positions, on the carbonate terminated plane) are vacant and, therefore, two methanoic acid molecules coordinate to one calcium atom, while a third methanoic acid coordinates to another calcium atom. Two of the methanoic acid molecules orientate in such a way that both the C–H and O–H hydrogen atoms are coordinated to oxygen atoms of the same surface carbonate group. The other methanoic acid molecule is orientated with its hydroxyl group away from the surface and its C–H hydrogen atom towards an oxygen atom of a surface carbonate group. On the carbonate terminated surface ($0.53\,J\,m^{-2}$), the methanoic acid molecules again coordinate via their C = O oxygen atom to calcium atoms just below the plane of the surface (Fig. 2). They attach in two parallel rows with Ca–O distances of 2.18 and 2.26 Å. The O–H hydrogen atoms of one of the rows of methanoic acid molecules are coordinated towards oxygen atoms of surface carbonate groups, the O–H hydrogen atoms of the other row are directed towards the C = O oxygen atoms of the other row of adsorbed molecules. The C–H hydrogen atoms are pointing away from the surface.

The dipolar {10$\bar{1}$1} surface shows similar behaviour to the {0001} surface, with the carbonate-terminated surface ($0.48\,J\,m^{-2}$) being stabilised much more than the calcium-terminated surface ($0.72\,J\,m^{-2}$). On the carbonate-terminated plane (Fig. 3) two of the adsorbed methanoic acid molecules move into the carbonate vacancies created when removing the dipole. These methanoic acid molecules are closely coordinated to the calcium ions of the lattice, via both their oxygen atoms, at similar Ca–O distances as those of the crystal lattice. The O–H hydrogen atom is situated at a position where a calcium atom would normally be in the crystal lattice. One of the other adsorbed methanoic acid molecules coordinates via its C = O oxygen atom to this hydrogen atom as it normally would to a calcium atom. The O–H hydrogen atom of this second molecule is coordinated to oxygen atoms of surface carbonate groups, and the C–H hydrogen atom is directed away from the surface. The rest of the methanoic acid molecules per unit cell coordinate via their C = O oxygen atom to calcium atoms just below the plane of the surface with a Ca–O distance of 2.22 Å. Both of the methanoic acid hydrogen atoms of this molecule point away from the surface. On the

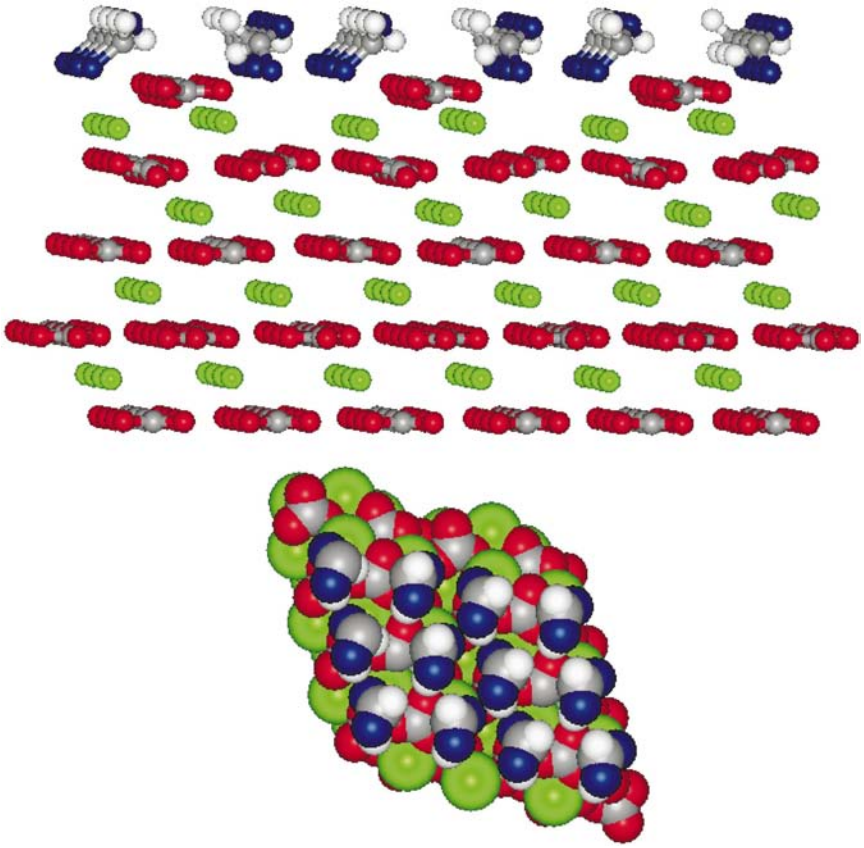

FIGURE 2 (a) Side view. (b) Plan view of the carbonate terminated {0001} surface with adsorbed methanoic acid molecules. Key: Ca = green; C = grey; O (carbonate) = red; O (methanoic acid) = blue; and H = white.

calcium terminated $\{10\bar{1}1\}$ surface, all the adsorbed methanoic acid molecules attach via their C = O oxygen atoms to surface calcium atoms, with Ca–O distances ranging from 2.17 to 2.43 Å. Three of the C–H hydrogen atoms are pointing away from the surface while the fourth is parallel to the plane of the surface. All the O–H hydrogen atoms are pointing towards oxygen atoms of surface carbonate groups with H–O distances of between 2.42 and 2.50 Å.

On the $\{11\bar{2}0\}$ surface, the methanoic acid molecules adsorb onto the surface in two rows. Because the lattice spacing between the calcium atoms of the $\{11\bar{2}0\}$ surface is small enough, the methanoic acid molecules in one of the rows are able to bridge two surface calcium atoms, via both their oxygen atoms. The methanoic acid molecules in the other row coordinate via

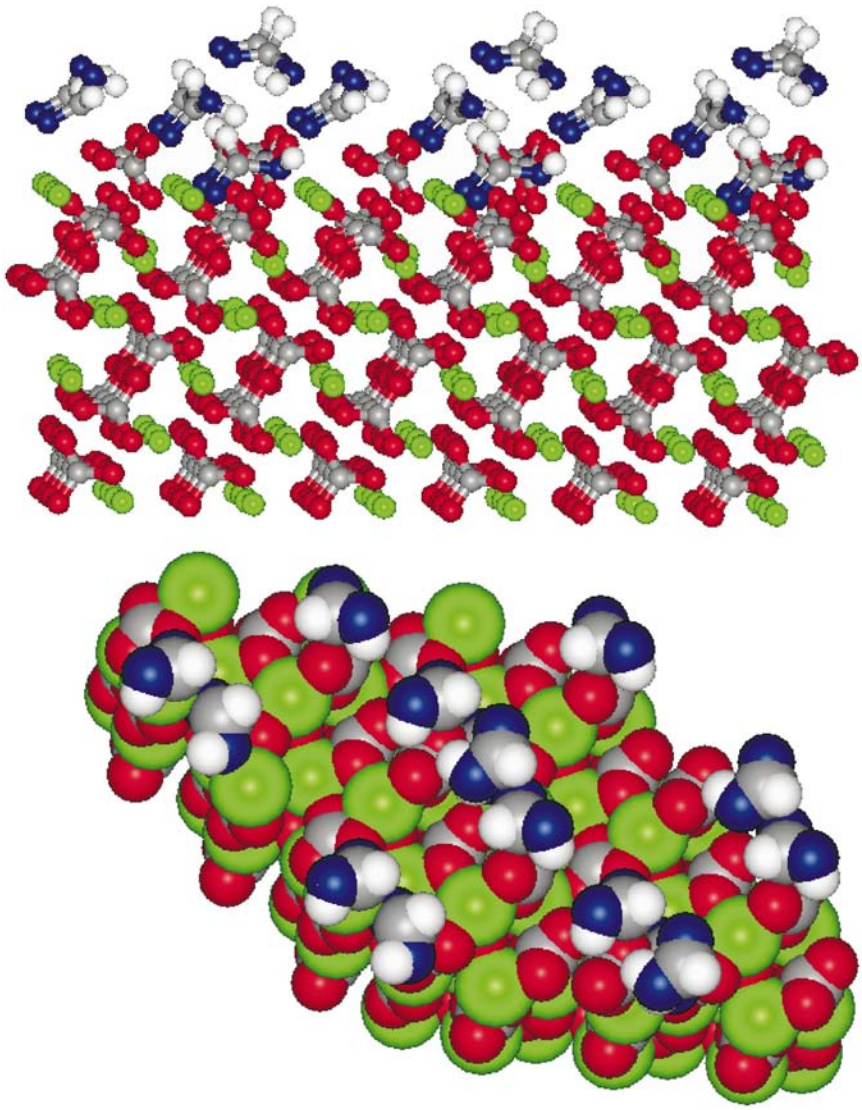

FIGURE 3 (a) Side view. (b) Plan view of the relaxed carbonate terminated $\{10\bar{1}1\}$ surface, showing some of the methanoic acid molecules occupying the vacancies due to removal of dipole. Key: Ca = green; C = grey; O (carbonate) = red; O (methanoic acid) = blue; and H = white.

their C = O oxygen atoms to one surface calcium atom each, with the O–H hydrogen atom in this case directed towards a surface oxygen atom. The C–H hydrogen atom for all the methanoic acid molecules is pointed away from the surface plane.

The methanoic acid molecules all adsorb onto the $\{10\bar{1}0\}$ surface via their C = O oxygen atoms to surface calcium atoms at Ca–O distances of between 2.17 and 2.20 Å. All the O–H hydrogen atoms are coordinated to surface oxygen atoms of carbonate groups at O–H distances of between 2.51 and 2.57 Å, and all the C–H hydrogen atoms point away from the plane of the surface.

The adsorption energies shown in Table I are all large and negative. The energy of adsorption of methanoic acid onto the $\{11\bar{2}0\}$ surface ($-112.9\,\mathrm{kJ\,mol^{-1}}$) is considerably larger than for the other surfaces, which is due to the lattice spacing of calcium atoms being small enough to allow each methanoic acid molecule to bridge two surface calcium atoms. The adsorption energy for the carbonate terminated $\{10\bar{1}1\}$ surface is also larger than the rest ($-90.0\,\mathrm{kJ\,mol^{-1}}$), which arises because half the adsorbed methanoic acid molecules are able to fill surface vacancies due to removal of the dipole in the dipolar surface. The rest of the adsorption energies are very similar and fall in the range of -44 to $-65\,\mathrm{kJ\,mol^{-1}}$, indicating physisorption of the methanoic acid molecules onto the surface.

Aragonite

Aragonite has an orthorhombic crystal structure with space group *Pmcn*. We started from the experimental structure found by Dickens and Bowen [40] with $a = 4.9598$ Å, $b = 7.9641$ Å, $c = 5.7379$ Å, $\alpha = \beta = \gamma = 90°$, which upon relaxation gave $a = 4.8314$ Å, $b = 7.8359$ Å, $c = 5.7911$ Å, $\alpha = \beta = \gamma = 90°$. We then cut the crystal to give the low index surfaces {001}, {010}, {100}, {011}, {110}, {101} and {111}, including the {010}, {011} and {110} surfaces, which are generally the surfaces expressed in the experimental morphology [41]. The seven aragonite surfaces considered in this work all have more than one termination giving a total of 17 surfaces to be investigated. In this work, we have concentrated on those surface terminations that are the most stable under aqueous conditions [18]. These planes will, therefore, be expressed in the crystal morphology in a growth/dissolution environment and will occur under the conditions of mineral separation processes. Table II lists the surface energies of these planes for the pure surface, and after the adsorption of methanoic acid.

After the adsorption of methanoic acid, the {001} surface has become the most stable surface, with a surface energy of $0.50\,\mathrm{J\,m^{-2}}$. The methanoic acid molecules attach via their C = O oxygen atoms to one surface calcium atom each. They coordinate in a regular pattern of two parallel rows with Ca–O distances of 2.22 and 2.29 Å. The O–H hydrogen atoms are coordinated to surface oxygen atoms, and each surface carbonate group bridges two hydrogen

TABLE II Surface energies for pure aragonite surfaces and after adsorption of methanoic acid

Surface	Surface energy ($J\,m^{-2}$)		Coverage (no. $HCOOH\,nm^{-2}$)	Adsorption energy ($kJ\,mol^{-1}$)
	Pure surface	After adsorption of methanoic acid		
{010}	1.50	0.64	4.4	−82.53
{001}	0.96	0.59	5.4	−42.36
{111}	0.84	0.53	4.6	−40.70
{011}	0.88	0.52	4.7	−46.58
{110}	0.99	0.70	3.4	−51.91
{101}	0.99	0.51	4.2	−67.78
{100}	0.85	0.50	5.3	−40.63

atoms. The C–H hydrogen atoms are angled away from the surface for all adsorbed molecules (Fig. 4).

Followed very closely in stability is the {011} surface which shows all four methanoic acid molecules orientated in different ways (Fig. 5). One coordinates via its C = O oxygen atom, but with both the O–H hydrogen atom and C–H

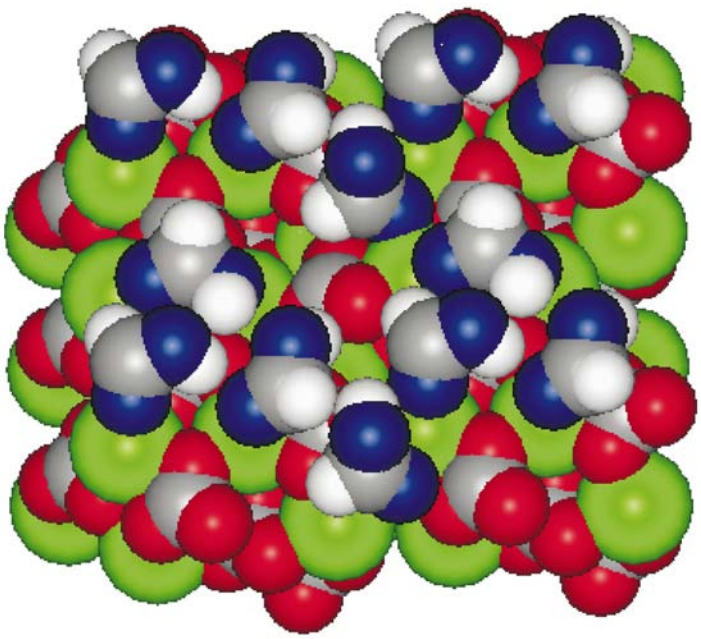

FIGURE 4 Plan view of the relaxed structure of the aragonite {001} surface, showing the methanoic acid molecules coordinated in two rows. Key: Ca = green; C = grey; O (carbonate) = red; O (methanoic acid) = blue; and H = white.

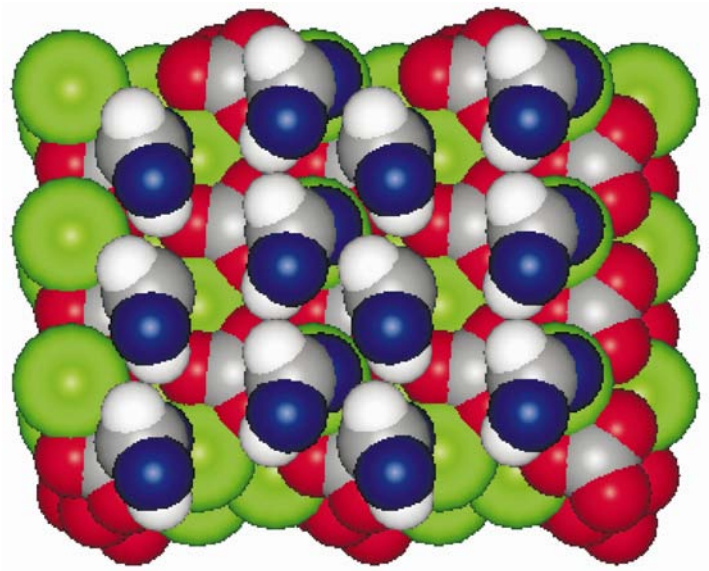

FIGURE 5 Plan view of the aragonite {011} surface, with all four methanoic acid molecules per unit cell adsorbed in different ways. Key: Ca = green; C = grey; O (carbonate) = red; O (methanoic acid) = blue; and H = white.

hydrogen atom directed away from the surface. One coordinates only via its O–H hydrogen atom to a surface oxygen atom, with both the C = O oxygen atom and the C–H hydrogen atom away from the surface. The third coordinates via both oxygen atoms to surface calcium atoms with the C–H hydrogen atom pointing away from the surface, and the last methanoic acid molecule interacts via the C = O oxygen atom, with the O–H hydrogen atom directed towards a surface oxygen atom and the C–H hydrogen atom angled away from the plane of the surface.

Although the {010} surface only has two surface calcium atoms per unit cell, it still manages to adsorb three methanoic acid molecules per cell. Two methanoic acid molecules adsorb to one of the surface calcium atoms, again via their C = O oxygen atoms, at Ca–O distances of 2.17 and 2.24 Å. The O–H hydrogen atoms for both these molecules are towards oxygen atoms of surface carbonate groups, with one of the C–H hydrogen atoms directed towards a surface oxygen atom and the other one pointing away from the surface. The other methanoic acid molecule per unit cell coordinates to the second available calcium atom, but sticks up almost perpendicular to the surface, with its O–H hydrogen directed towards a surface oxygen atom, and its C–H hydrogen pointing directly away from the surface.

The {110} surface has a large enough unit cell to accommodate five methanoic acid molecules per unit cell. Since there are only four calcium atoms per unit cell available for the methanoic acid molecules to interact with, two of the methanoic acid molecules coordinate to the same calcium atom, with the other three surface calcium atoms adsorbing one each. Ca–O distances are between 2.16 and 2.44 Å. Two of the O–H hydrogen atoms are angled away from the surface, with three directed towards surface oxygen atoms, at O–H distances of between 2.41 and 2.44 Å. Only two C–H hydrogen atoms are now angled away from the surface, the other three point towards surface oxygen atoms, each directed between two oxygen atoms of the same carbonate group at O–H distances of between 2.59 and 2.74 Å, which is too far for formal hydrogen bonding.

The {111} surface has the largest surface area of the surfaces considered and it manages to adsorb six methanoic acid molecules per cell. All of the adsorbed molecules coordinate via their C = O oxygen atoms to surface calcium atoms, Ca–O distances ranging between 2.17 and 2.48 Å. All the O–H hydrogen atoms are directed towards oxygen atoms of surface carbonate groups at O–H distances of between 2.43 and 2.55 Å and all of the C–H hydrogen atoms are pointing away from the surface.

On the {101} surface, three of the methanoic acid molecules that adsorb per unit cell interact as before via their C = O oxygen to a surface calcium atom. The fourth methanoic acid molecule coordinates via the O–H oxygen atom, again to a surface calcium atom. The O–H hydrogen atom of this molecule is pointing away from the surface, as is the C = O oxygen atom, while the C–H hydrogen atom is parallel to the surface. The O–H hydrogen atoms of the other three methanoic acid molecules point towards surface oxygen atoms.

The last of the surfaces considered, the {100} surface, has all the methanoic acid molecules coordinating via their C = O oxygen atoms to surface calcium atoms. All four methanoic acid molecules per unit cell attach with slightly different orientations. The Ca–O distances range from 2.23 to 2.34 Å. Three of the O–H hydrogen atoms are orientated towards surface oxygen atoms at distances of between 2.35 and 2.41 Å, while the hydroxyl group of the fourth methanoic acid adsorbate is pointing away from the surface. The C–H hydrogen atom of this fourth molecule is directed between two surface oxygen atoms of separate carbonate groups, while the other three C–H hydrogen atoms are angled away from the plane of the surface.

As with the calcite surfaces, all of the adsorption energies for methanoic acid are large and negative. The values range from $-41\,\mathrm{kJ\,mol^{-1}}$ for the {001} surface to $-83\,\mathrm{kJ\,mol^{-1}}$ for the {100} surface, again indicating physisorption of the methanoic acid molecules to the aragonite surfaces.

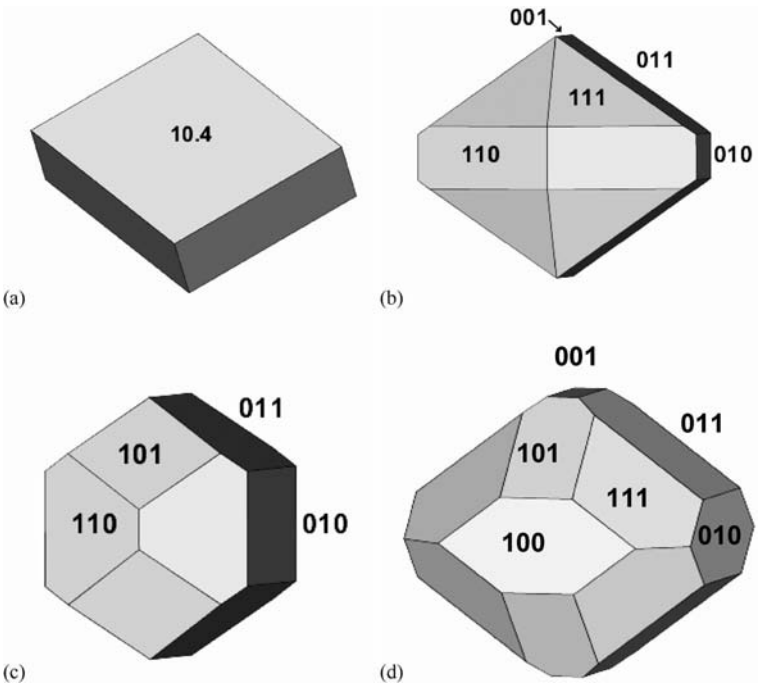

FIGURE 6 Equilibrium morphologies of (a) calcite, either hydrated or covered by a monolayer of methanoic acid, (b) dry aragonite, (c) hydrated aragonite and (d) aragonite after adsorption of methanoic acid at the surfaces.

MORPHOLOGY

Wulff [42] and Gibbs [43] showed that equilibrium morphologies of minerals can be obtained from their surface energies and we investigated whether the morphologies of calcite and aragonite are changed by the adsorption of methanoic acid onto their surfaces, by comparing the morphologies of the dry and hydrated minerals [26] with those calculated from the surface energies after adsorption of methanoic acid. The equilibrium morphology of calcite is shown in Fig. 6(a), which is the same as for the hydrated crystal or after adsorption of methanoic acid, due to the exceptional stability of the $\{10\bar{1}4\}$ surface under these conditions. However, the morphology of aragonite does show changes when the environment is altered. Fig. 6(b) shows the morphology of the dry aragonite crystal, which changes considerably upon hydration, shown in Fig. 6(c) [26]. We see that upon hydration of the mineral surfaces, the relative stabilities of the {101} and {010} surfaces are increased, mainly at the expense of the {111} surface, which is no longer expressed in the morphology, in agreement with the

experimental crystal morphology [40]. When methanoic acid is adsorbed onto the surface, the morphology is altered again, shown in Fig. 6(d), differing considerably from both the dry and hydrated equilibrium morphologies. The main feature of the new crystal shape is the appearance of the {100} and {111} surfaces, which, compared to the hydrated morphology, have been stabilised with respect to the other surfaces, while the {110} surface is no longer expressed in the morphology. Instead of being elongated, the aragonite mineral has also become more spherical and if we look at the surface energies of the surfaces with adsorbed methanoic acid (Table II), we see that the effect of adsorbing methanoic acid onto the surfaces is to even out the relative surface energies, resulting in the spherical equilibrium morphology, where all surfaces are expressed to a similar extent (apart from the {110} surface, which has the highest surface energy). The morphology shown in Fig. 6(d) is, of course, the extreme case, where all aragonite surfaces are covered with a monolayer of methanoic acid. This is unlikely to occur in nature, but we suggest that in the presence of methanoic or similar carboxylic acids, the morphology of the hydrated aragonite mineral will be modified to a greater or lesser extent, depending on concentration and relative energies of adsorption, in line with the trends shown in Fig. 6(d).

CONCLUSION

We have modelled the adsorption of methanoic acid onto a series of calcite and aragonite surfaces. As a result, we find that the stability of the low index surfaces of both calcite and aragonite are significantly affected by the adsorption of methanoic acid. All the surfaces considered were stabilised by adsorption of methanoic acid, especially the dipolar surfaces of calcite where the carbonate-terminated surface becomes far more stable than the calcium-terminated plane. This increased stability of the carbonate planes can be attributed to the methanoic acid molecules filling the carbonate vacancies, created when the dipole was removed.

On all but a few of the calcite and aragonite surfaces, the methanoic acid molecules coordinate to the surface via their double bonded oxygen to either one surface calcium atom, or bridging two where the orientation of the surface calcium atoms allows, with Ca–O distances ranging from 2.17 to 2.28 Å. In addition, there is usually significant coordination between the hydrogen atoms of the hydroxyl group of the methanoic acid molecules and oxygen atoms of one of the carbonate groups of the surface, with O–H distances of between 2.42 and 2.82 Å.

Generally, the hydrogen atom bonded to the carbon of the methanoic acid molecules is directed away from the surface. This configuration is of considerable significance since we are using methanoic acid as a model adsorbate for long chain carboxylic acid collector molecules, such as oleic acid, which are used in the process of flotation. Since the hydrogen atoms bonded to the carbon of the methanoic acid carbon atoms are directed away from the surface, the replacement with a long chain hydrocarbon might result in crosslinking and/or other interactions between the adsorbates, but the polar head group is not significantly changed and, hence, we would expect that the adsorption energies for oleic acid onto calcite and aragonite surfaces will be similar to those calculated here for methanoic acid.

The equilibrium morphology of calcite is not altered by the adsorption of methanoic acid onto the surfaces, but the aragonite morphology is changed considerably. The {100} and {111} surfaces have been stabilised and are now expressed in the new morphology at the expense of the {110} surface, which has completely disappeared from the morphology. The crystal shape has become spherical due to the similarity of the surface energies of the different aragonite surfaces, once a monolayer of methanoic acid has been adsorbed.

Future work will include modelling the adsorption of organic molecules with different functional groups and molecular dynamics simulations to include temperature into the calculations. In addition, we will investigate co-existing minerals, such as fluorite, to calculate relative strengths of adsorption of the surfactant molecules to different minerals.

Acknowledgements

We thank the Engineering and Physical Research Council, Grant No. GR/N65172/01, and the Royal Society, Grant No. 22292 for their financial support.

References

[1] Park, N.S., Kim, M.W., Langford, S.C. and Dickinson, J.T. (1996) "Atomic layer wear of single-crystal calcite in aqueous solution scanning force microscopy", *J. Appl. Phys.* **80**, 2680.
[2] Cabezon, L.M., Caballero, M. and Perez-Bustamante, J.A. (1994) "Coflotation separation for the determination of heavy-metals in water using colloidal gas aphrons system", *Sep. Sci. Technol.* **29**, 1491.
[3] Beruto, D. and Giordani, M. (1993) "Calcite and aragonite formation from aqueous hydrogen carbonate solutions—effect of induced electromagnetic-field on the activity of $CaCO_3$ nuclei precursors", *J. Chem. Soc., Faraday Trans.* **89**, 2457.
[4] Goni, S., Sobrado, L. and Hernandez, M.S. (1993) "Increase of acid–surface reactivity through water molecules adsorption process: V_2O_5–$CaCO_3$ behaviour", *Solid State Ionics* **63**, 786.

[5] Stipp, S.L. and Hochella, M.F. (1991) "Structure and bonding environments at the calcite surface as observed with photoelectron–spectroscopy (XPS) and low-energy electron-diffraction", *Geochim. Cosmochim. Acta* **55**, 1723.
[6] Stipp, S.L., Gutmannsbauer, W. and Lehmann, T. (1996) "The dynamic nature of calcite surfaces in air", *Am Mineral.* **81**, 1.
[7] Liang, Y., Lea, A.S., Baer, D.R. and Engelhard, M.H. (1996) "Structure of the cleaved $CaCO_3$ surface in an aqueous environment", *Surf. Sci.* **351**, 172.
[8] Gratz, A.J., Hillner, P.E. and Hansma, P.K. (1993) "Step dynamics and spiral growth on calcite", *Geochim. Cosmochim. Acta* **57**, 491.
[9] Wright, K., Cygan, R.T. and Slater, B. (2001) "Structure of the (10(1) over-bar4) surfaces of calcite, dolomite and magnesite under wet and dry conditions", *Phys. Chem. Chem. Phys.* **3**, 839.
[10] de Leeuw, N.H. and Parker, S.C. (1998) "Modeling the competitive adsorption of water and methanoic acid on calcite and fluorite surfaces", *Langmuir* **14**, 5900.
[11] de Leeuw, N.H., Parker, S.C. and Harding, J.H. (1999) "Molecular dynamics simulation of crystal dissolution from calcite steps", *J. H. Phys. Rev. B* **60**, 13792.
[12] Liang, Y., Baer, D.R., McCoy, J.M., Amonette, J.E. and LaFemina, J.P. (1996) "Dissolution kinetics on the calcite–water interface", *Geochim. Cosmochim. Acta* **60**, 4883.
[13] McCoy, J.M. and LaFemina, J.P. (1997) "Kinetic Monte Carlo investigation of pit formation at the $CaCO_3$ (10(1) over-bar4) surface–water interface", *Surf. Sci.* **373**, 288.
[14] Fenter, P. and Sturchio, N.C. (1999) "Structure and growth of stearate monolayers on calcite: first results of an *in situ* X-ray reflectivity study", *Geochem. Cosmochim. Acta* **63**, 3145.
[15] Madsen, L., GrahlMadsen, L., Gron, C., Lind, I. and Engell, J. (1996) "Adsorption of polar aromatic hydrocarbons on synthetic calcite", *Org. Geochem.* **24**, 1151.
[16] Zouboulis, A.I., Zamboulis, D. and Matis, K.A. (1991) "Foam flotation of zeolites—application for zinc ion removal", *Sep. Sci. Technol.* **26**, 355.
[17] Loewenberg, M. and Davis, R.H. (1994) "Flotation rates of fine, spherical-particles and droplets", *Chem. Eng. Sci.* **49**, 3923.
[18] Miller, J.D., Yalamanchili, M.R. and Kellar, J.J. (1992) "Surface-charge of alkali-halide particles as determined by laser-Doppler electrophoresis", *Langmuir* **8**, 1464.
[19] Armstrong, D.W., Zhou, E.Y., Chen, S., Le, K. and Tang, Y. (1994) "Foam flotation enrichment of enantiomers", *Anal. Chem.* **66**, 4278.
[20] Ince, D.E., Johnston, C.T. and Moudgil, B.M. (1991) "Fourier-transform infrared spectroscopic study of adsorption of oleic acid oleate on surfaces of apatite and dolomite", *Langmuir* **7**, 1453.
[21] De Castro, F.H.B. and Borrego, A.G. (1995) "Modification of surface-tension in aqueous-solutions of sodium oleate according to temperature and pH in the flotation bath", *J. Colloid. Interface Sci.* **173**, 8.
[22] Ghazy, S.E., Kabil, M.A., Abeidu, A.M. and El-Metwally, N.M. (1996) "Selective separation of magnesium from olivine minerals", *Sep. Sci. Technol.* **31**, 829.
[23] Hancer, M. and Celik, S. (1993) "Flotation mechanisms of boron minerals", *Sep. Sci. Technol.* **28**, 1703.
[24] Didymus, J.M., Oliver, P., Mann, S., De Vries, A.L., Hauschka, P.V. and Westbroek, P. (1993) "Influence of low-molecular-weight and macromolecular organic additives on the morphology of calcium carbonate", *J. Chem. Soc., Faraday Trans.* **89**, 2891.
[25] Oliver, P.M., Parker, S.C. and Mackrodt, W.C. (1993) "Computer simulation of the crystal morphology of NiO", *Model. Simul. Mater. Sci. Eng.* **1**, 755.
[26] de Leeuw, N.H. and Parker, S.C. (1998) "Surface structure and morphology of calcium carbonate polymorphs calcite, aragonite, and vaterite: an atomistic approach", *J. Phys. Chem. B* **102**, 2914.
[27] Parker, S.C., Kelsey, E.T., Oliver, P.M. and Titiloye, J.O. (1993) "Computer modeling of inorganic solids and surfaces", *Faraday Discuss.* **95**, 75.
[28] Davies, M.J., Parker, S.C. and Watson, G.W. (1994) "Atomistic simulation of the surface-structure of spinel", *J. Mater. Chem.* **4**, 813.
[29] Purton, J., Bullett, D.W., Oliver, P.M. and Parker, S.C. (1995) "Electronic structure and atomistic simulations of the ideal and defective surfaces of rutile", *Surf. Sci.* **336**, 166.
[30] de Leeuw, N.H. and Parker, S.C. (1997) "Atomistic simulation of the effect of molecular adsorption of water on the surface structure and energies of the calcite surfaces", *J. Chem. Soc., Faraday Trans.* **93**, 467.

[31] de Leeuw, N.H., Watson, G.W. and Parker, S.C. (1995) "Atomistic simulation of the effect of dissociative adsorption of water on the surface structure and stability of calcium and magnesium oxide", *J Phys. Chem.* **99**, 17219.
[32] de Leeuw, N.H., Watson, G.W. and Parker, S.C. (1996) "Atomistic simulation of adsorption of water on three-, four-, and five-coordinated surface sites of magnesium oxide", *J. Chem. Soc., Faraday Trans.* **92**, 2081.
[33] Born, M. and Huang, K. (1954) Dynamical Theory of Crystal Lattices (Oxford University Press, Oxford).
[34] Dick, B.G. and Overhauser, A.W. (1958), *Phys. Rev.* **112**, 90.
[35] Pavese, A., Catti, M., Parker, S.C. and Wall, A. (1996) "Modelling the thermal dependence of structural and elastic properties of calcite, $CaCO_3$", *Phys. Chem. Miner.* **23**, 89.
[36] Osguthorpe, P., Osguthorpe, D. and Hagler, A. (1988), *Proteins; Structure, Function and Genetics* **14**, 786.
[37] Watson, G.W., Kelsey, E.T., de Leeuw, N.H., Harris, D.J. and Parker, S.C. (1996) "Atomistic simulation of dislocations, surfaces and interfaces in MgO", *J. Chem. Soc., Faraday Trans.* **92**, 433.
[38] Tasker, P.W. (1979) "The surface energies, surface tensions and surface structure of the alkali halide crystals", *Philos. Mag. A.* **39**, 119.
[39] Lide, D.R. (1994) Handbook of Chemistry and Physics (CRC Press Inc. Boca Raton, USA).
[40] Dickens, B. and Bowen, J.S. (1971), *J. Res. Natl. Bur. Stand., Sect A: Phys. Chem.* **75**, 27.
[41] Dana, E.S. (1958) A Textbook of Mineralogy (John Wiley & Sons, New York).
[42] Wulff, G. (1901), *Z. Kristallogr. Kristallgeom.* **34**, 949.
[43] Gibbs, J.W. (1928) Collected Works (Longman, New York).